ELSEVIER

Journal of Materials Processing Technology 68 (1997) 33–38

Journal of Materials Processing Technology

A simple algorithm for stamping circular plates by hemispherical punches

M. Kadkhodayan, L.C. Zhang *

Centre for Advanced Materials Technology, Department of Mechanical and Mechatronic Engineering, The University of Sydney, Sydney, NSW 2006, Australia

Received 6 October 1995

Abstract

This paper proposes a simple algorithm for solving the contact problems in relation to sheet stamping. The efficiency and reliability of the algorithm are demonstrated by an investigation of the stamping of elastic–plastic circular plates into a conical die with a hemispherical rigid punch. The analysis shows that the contact stress varies greatly with the punch displacement and deviates from the uniform distribution used for approximate analyses. It is found that the central gap between the punch and the plate surfaces does not disappear before coining. Using the proposed algorithm, the applicable range of the small deflection theory of plate bending has been examined, revealing that the applicable range of this theory is much smaller than is usually thought.

Keywords: Elastic–plastic deformation; Contact problem; Sheet stamping; Circular plate

1. Introduction

Stamping sheet metals into dies is one of the most commonly used manufacturing processes in production engineering. However, to design the forming tools properly, the deformation mechanisms of a workpiece must be taken into account.

The axisymmetric stamping of sheet metals by hemispherical punches is a typical process in practice and is also a characterised test for evaluating the formability of sheet metals. Johnson and Singh [1] studied the problem experimentally and found that the springback of a circular plate increases as the radius of the plate decreases, and that a central gap between the punch and plate exists. Yu and Johnson [2] presented an analytical solution using an analogy between a linear elastic beam and a rigid/linear work-hardening beam beyond yield. Later, Yu, Johnson and Stronge [3,4] extended the above study by assuming that the plate material was either perfectly elastic or rigid–perfectly plastic, to avoid mathematical difficulties dividing the plate into a central and an outer portion and considering that the former follows precisely the surface profile of the punch and that the latter has a conical shape. Assuming that the interaction between the punch and plate surfaces can be replaced by a concentrated ring load, Zhang, Yu and Wang [5] analysed the stamping process with a conical die. The variation of the ring load radius was accommodated by an experimental relationship. According to the experimental study of Lu and Ong [6], however, the contact-force distribution between the punch and plate will deviate largely from a ring load when the plate is deformed considerably. Recently, Kormi et al. [7] tried to simulate the process by the finite-element method, but their results were not consistent with experimental observations [1,5,6].

The present paper proposes a simple but reliable algorithm for the axisymmetric stamping of circular sheet by a hemispherical punch. The applicable range of small and large deflection theories of plate bending to this type of problems is explored.

* Corresponding author. Fax: +61 2 93513760; e-mail: zhang@tiny.me.su.oz.au

0924-0136/97/$17.00
PII S0924-0136(96)02524-1

2. Algorithm for elastic–plastic contact problems

2.1. Solution strategy

Consider the contact between two bodies, a rigid punch and a deformable plate, which is described by the compatibility conditions:

$$g \geq 0, \quad q \leq 0, \quad gq = 0, \tag{1}$$

where g is the gap between the surfaces of the punch and plate at a point and q is the normal contact stress at the point. The above conditions indicate that: (i) the plate cannot penetrate into the punch; and (ii) the contact stress is compressive for a pair of points in contact, but zero for others.

In solving an elastic–plastic contact problem, the increment of the external load or displacement is controlled by the smallest value of the following governing factors. (1) r_1: the extent of plasticity; (2) r_2: the maximum strain increment; (3) r_3: the maximum rotation increment; (4) r_4: the penetration condition; and (5) r_5: the separation condition.

The first three factors concern the monitoring of the deformation of the plate and the last two are for contact adjustment. For example, when the stress at a point in the plate is greater than the yield stress, r_1 should be computed to ascertain the stress state of the yielding surface. Nevertheless, r_4 must be calculated to prevent the penetration of the plate into the punch. In addition, since the plate does not adhere to the punch, a contact point may be separated from the punch surface. Hence, r_5 needs to be assigned to ensure zero force at a point without contact.

Factors r_1, r_2 and r_3 can be determined properly by the consistent elastic–plastic algorithm [8]. However, the increment of the external load or displacement should be controlled by the smallest value of r_4 and r_5, as described below.

The plate is first divided into finite-difference meshes, thus only a finite number of nodes need to be considered in the contact treatment. These nodes are of two types: contact nodes and free nodes. The contact force on a pair of nodes in contact is unknown in advance but is a function of the incremental nodal displacement and the resultant forces, i.e.:

$$\delta q = f(w, \delta w, \delta M_r, \delta M_\theta), \tag{2a}$$

when the small deflection theory of plate bending is used, or:

$$\delta q = f(w, \delta w, N_\theta, \delta N_\theta, N_r, \delta N_r, \delta M_r, \delta M_\theta), \tag{2b}$$

when the large deflection theory is employed. In the above equations, w, M_r, M_θ, N_r and N_θ are deflection, bending moments and membrane forces in the radial and circumferential directions, respectively.

Now, if $\Psi^J = 0$ describes the profile of the punch surface at the J-th displacement step, then the corresponding displacements for all of the contact nodes must satisfy this instant surface equation. For free nodes, the contact forces are zero and no displacement constraint applies. In an incremental displacement scheme, a displacement increment $\delta\Delta^J$ is applied to the punch at the J-th step. After a calculation of the plate deformation, the converged results must be analysed to examine the current contact state and to see if the applied incremental displacement needs to be re-examined. If neither penetration nor traction force is observed, the obtained deformation state is correct; otherwise, $\delta\Delta^J$ must be amended and the whole calculation repeated. The instant resultant punch load can be calculated by integrating the contact stress over the contact zone. The above solution strategy can be presented more clearly by the following statement:

(a) *apply an incremental displacement* $\delta\Delta^J$,
(b) *find the deflection of the plate*,
(c) *if any penetration occurs, modify* $\delta\Delta^J$ *and return to step* (a) (*i.e., if* $(R_p - (d_i)_{min})/R_p > Tol_1 \Rightarrow \delta\Delta^J = (r_4)_{min}\delta\Delta^J$, *where* $(r_4)_{min} = (d_i)_{min}/R_p$; *otherwise continue*,
(d) *if any traction forces are detected, modify* $\delta\Delta^J$ *and return to step* (a) (*i.e., if* $(q_i)_{max} > 0$ *and* $|(q_i)_{max}/(q)^*_{max}| > Tol_2 \Rightarrow \delta\Delta^J = (r_5)_{min}\delta\Delta^J$, *where* $(r_5)_{min} = Tol_2/|(q_i)_{max}/(q_i)^*_{max}|$; *otherwise continue*,
(e) *update variables* (*e.g., stresses, strains and displacements*)).

In the above algorithm, R_p and d_i are the radius of the hemispherical punch and the distance between the centre of the punch and the i-th node on the plate, see Fig. 1. Quantities q_i and q_i^* are respectively the normal nodal force of contact on the i-th node at the current

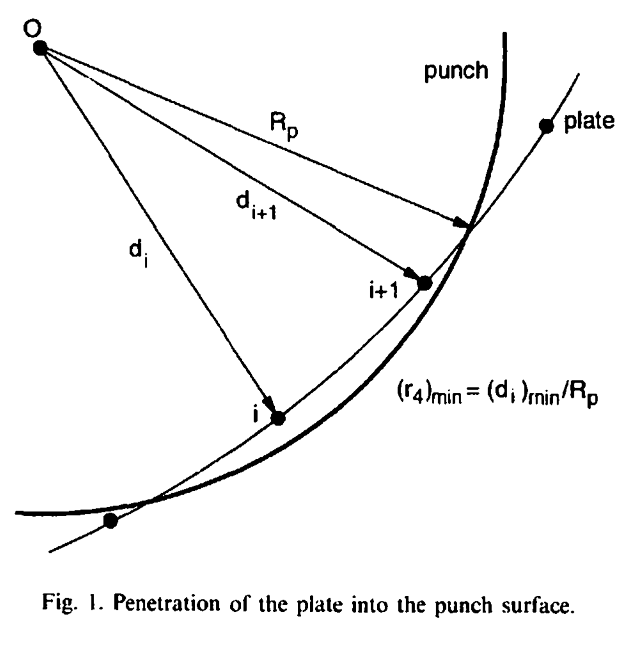

Fig. 1. Penetration of the plate into the punch surface.

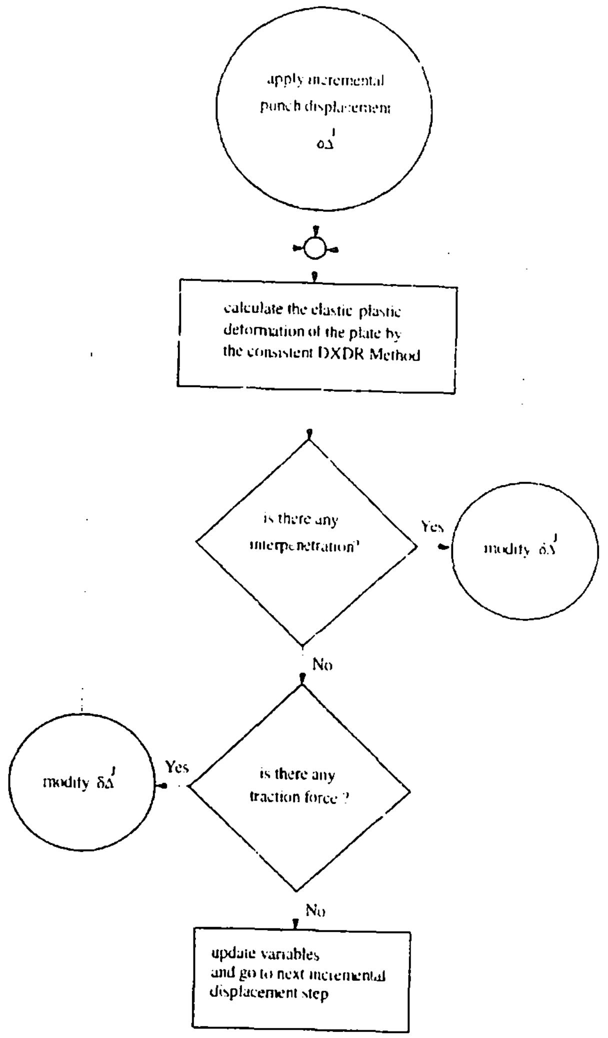

Fig. 2. Flowchart of the solution strategy.

iteration step and that at the converged incremental step $\delta\Delta^{J-1}$. Quantities Tol_1 and Tol_2 are the given tolerances for examining the penetration and traction of a node, the magnitudes of which depend on the computational accuracy required. ($Tol_1 = 0.002$ and $Tol_2 = 0.1$ were used throughout the calculation in this paper.) Quantities $(d_i)_{min}$ and $(q_i)_{max}$ in steps (c) and (d) are thus two indicators for the judgments. The modification of $\delta\Delta^J$ is based on the node with the maximum value of penetration or traction force. The associated flowchart of the solution strategy is shown in Fig. 2.

2.2. The algorithm

According to the above discussion, a complete algorithm for the elastic-plastic contact problem combined with the consistent DXDR method [8] can be obtained as follows:

(a) *$J = 1$, specify N_{max}, e_R, e_k, and Δ_{max}, where Δ is displacement of the punch, J is the number of the punch displacement step and e_R and e_k are the convergence indexes for kinetic energy and residual force, respectively;*
(b) *apply a new increment of punch displacement $\delta\Delta^J$;*
(c) *$\dot{X}^0 = 0$, $n = 0$; specify X^0;*
(d) *$\zeta_i^0 = 0$ ($i = 1, \ldots, N_{total}$); exert boundary conditions;*
(e) *determine $\tilde{X}^n$ and iterate if necessary;*
(f) *form* **M**;
(g) *compute $d\varepsilon^n$;*
(h) *if the node was elastic in the last load step, continue, otherwise turn to* (j);
(i) *if the node is still elastic (this must be true when $n = 0$), $d\sigma^n = d\sigma_e^n$, and turn to* (k); *if it becomes plastic, $d\sigma^n = (1 - \eta^n)d\sigma_e^n + \eta^n \mathbf{C}_{ep}^n d\varepsilon^n$ and turn to* (k), *where $\eta^n = (\bar{\sigma}_e^n - Y^n)/(\bar{\sigma}_e^n - \bar{\sigma}^n)$ is the proportional factor; if necessary, sub-incremental steps can be used in calculating $d\sigma^n$;*
(j) *if the node is still plastic (this must be true when $n = 0$), $d\sigma^n = \mathbf{C}_{ep}^n d\varepsilon^n$ (use sub-incremental steps if necessary), if it becomes elastic, $d\sigma^n = d\sigma_e^n$;*
(k) *temporarily update the stresses ($\sigma^{n+1} = \sigma^n + d\sigma^n$) and relevant variables;*
(l) *calculate the dis-equilibrium force $\boldsymbol{R}^n$;*
(m) *if $|R_i^{L,n}| \le e_R$ ($L = u$, v, w), turn to* (u); *otherwise continue;*
(n) *calculate ζ_i^n;*
(o) *obtain $\dot{\mathbf{X}}^{n+1/2}$;*
(p) *if $\sum_{L=u}^{w}\sum_{i=1}^{N}(\dot{x}_i^{L,n+1/2})^2 \le e_k$, turn to* (u); *otherwise continue;*
(q) *calculate X^{n+1};*
(r) *apply boundary conditions;*
(s) *calculate the contact forces;*
(t) *$n = n + 1$; if $n > N_{max}$, stop; otherwise return to step* (f);
(u) *update displacements and contact forces, temporarily;*
(v) *if any penetration occurs, $\delta\Delta^J = (d_i)_{min}\delta\Delta^J/R_p$ and return to* (c); *otherwise continue;*
(w) *if any traction forces are detected, $\delta\Delta^J = (Tol_2)\delta\Delta^J/|(q_i)_{max}/(q_i)^*_{max}|$ and return to* (c); *otherwise continue;*
(x) *update corresponding variables;*
(y) *if $\Delta > \Delta_{max}$ stop; otherwise, $J = J + 1$ and return to step* (b).

3. Application

3.1. Modelling of circular plates under axisymmetric stamping

As an application example of the above algorithm, consider the stamping of a circular plate pressed by a hemispherical punch in a conical die (Fig. 3). The

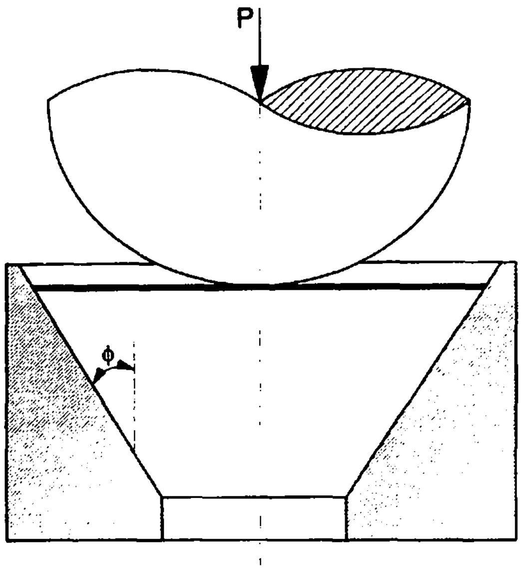

Fig. 3. The stamping process.

deformation of the plate can be modelled by the boundary value problem shown in Fig. 4. Assume that the friction coefficient between the plate periphery and the conical die surface is μ, that the friction between the surfaces of punch and plate is negligible and that the semi-angle of the die is ϕ. In Fig. 4(a), F_1 and F_2 are respectively the friction force and normal reaction on the plate due to the die. Hence, the boundary forces on the plate, N_R and M_R in Fig. 4(b), are:

$$\begin{cases} N_R = \dfrac{-P(\cos\phi - \mu\sin\phi)}{2\pi(R+u_R)(\sin\phi + \mu\cos\phi)}, \\ M_R = \dfrac{1}{2} h N_R, \end{cases} \quad (3)$$

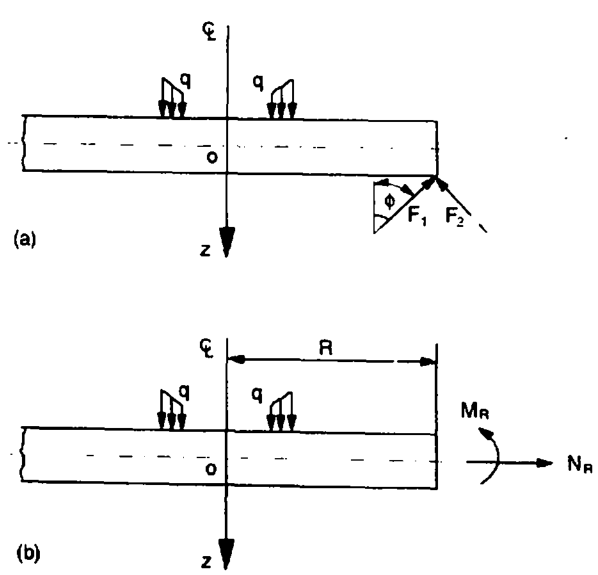

Fig. 4. Mechanical model of the workpiece.

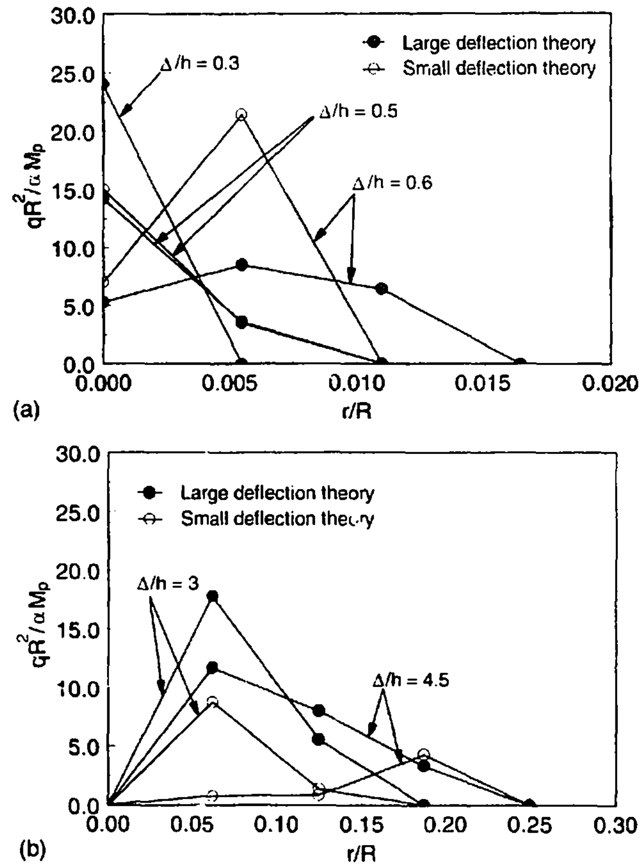

Fig. 5. Distribution of contact pressure for the elastic - plastic circular plate: (a) $\Delta/h \leq 0.6$; (b) $\Delta/h = 3$ and 4.5.

where h and R are the thickness and radius of the circular plate before deformation, respectively.

The plate deformation is analysed using both small and large deflection theories of bending. The plate material follows the simple J_2 flow theory of plasticity and the linear isotropic hardening rule. The material constants are Young's modulus $E = 196.2$ GPa, work-hardening modulus $E_t = 1.42$ GPa, Poisson's ratio $\upsilon = 0.2862$ and yield stress $Y = 201.1$ MPa. The plate is of radius $R = 75$ mm and thickness $h = 2$ mm. The diameter of the hemispherical punch is 200 mm. The semi-angle of the conical die is $\phi = 20°$ and the friction coefficient between the plate and die is $\mu = 0.2$.

3.2. Results and discussion

Fig. 5 demonstrates the interaction of the hemispherical punch with the circular plates. The distribution of the contact force varies significantly with the punch displacement (see the curves from the large deflection theory). When Δ/h is small, the plate centre is subjected to the maximum contact stress. It is clear from the figure that the contact stresses are very different from a locally-uniform distribution used for approximate analyses [3].

As the stamping proceeds, the contact stress at the plate centre decreases considerably and a central gap between the punch and plate surfaces appears when Δ/h reaches 2.8, Fig. 5(b) and Fig. 6. This is in agreement with earlier experimental observations [1,5,6].

The development of the central gap is shown more clearly in Fig. 6. The magnitude of the gap at the plate centre, g_c, increases rapidly with increasing bending, but approaches a constant value after Δ/h reaches 4. it is clear that the gap will not disappear before coining takes place. The appearance and development of the gap is controlled mainly by the material properties of the plate, which govern the variation of the plate curvature during bending.

The theoretical relationship between the external load P and the diameter of the contact zone d_c, and that between the punch displacement Δ and d_c, are in very good agreement with the experimental results [5,6], Fig. 7a and 7b, which confirms the accuracy and reliability of the proposed algorithm.

The applicable range of the small deflection theory to plate stamping can be examined by comparing its prediction with that from the large deflection theory. Fig. 8 shows the variation of the non-dimensional external load, $P/\alpha M_p$, with the non-dimensional punch displacement, Δ/h, for both elastic and elastic–plastic plates using small (S) and large (L) deflection theories. When $\Delta/h \leq 0.7$, all the solutions, both elastic and elastic–plastic, from small or large deflection theories, are very close to each other. In this regime, the effect of membrane forces is negligible and the plastic deformation is very localised, thus the overall deflection of the plate is controlled by the elastic properties of the material. However, if the prediction of the contact forces between the plate and punch is important, the small deflection theory is applicable only when $\Delta/h \leq 0.5$, beyond this the distribution of the contact forces given by the small deflection theory being totally wrong (Fig. 5).

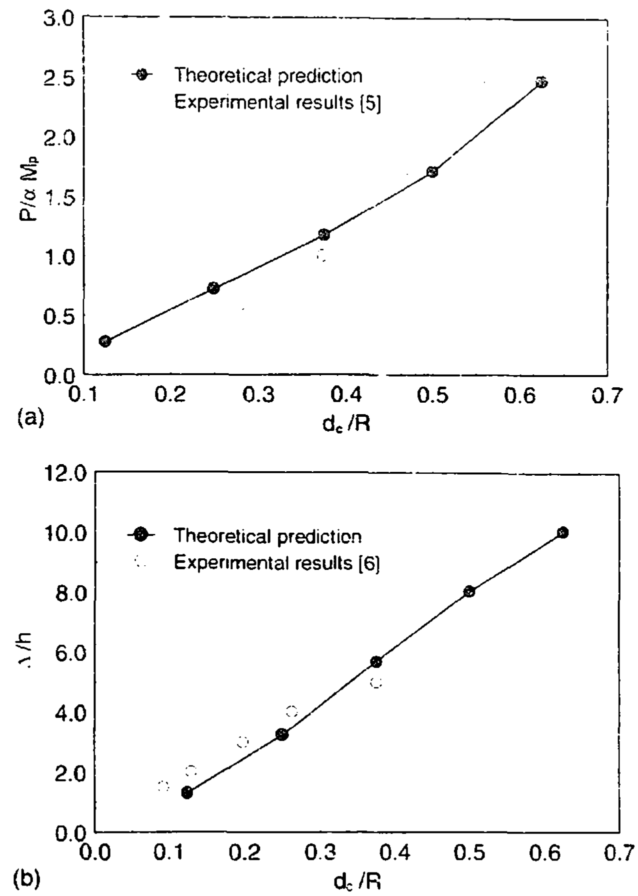

Fig. 7. Variation of contact zone diameter in the large deflection elastic–plastic plate: (a) with external load: (b) with punch displacement.

4. Conclusions

1. An efficient algorithm for solving contact problems associated with elastic–plastic stamping of circular plates has been proposed. The algorithm is reliable and can be extended for further complex stamping problems.

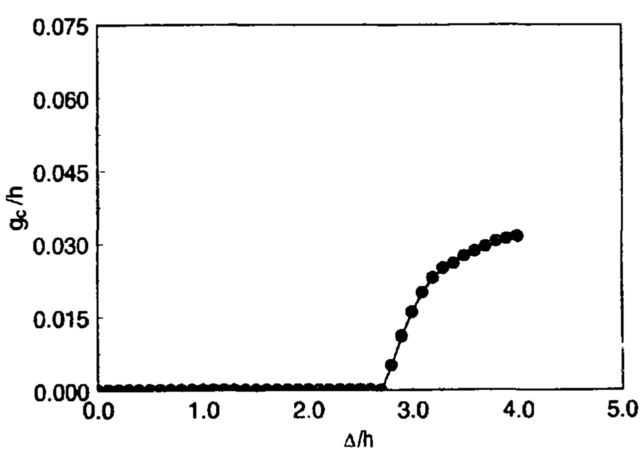

Fig. 6. Development of a central gap between the punch and the plate surface.

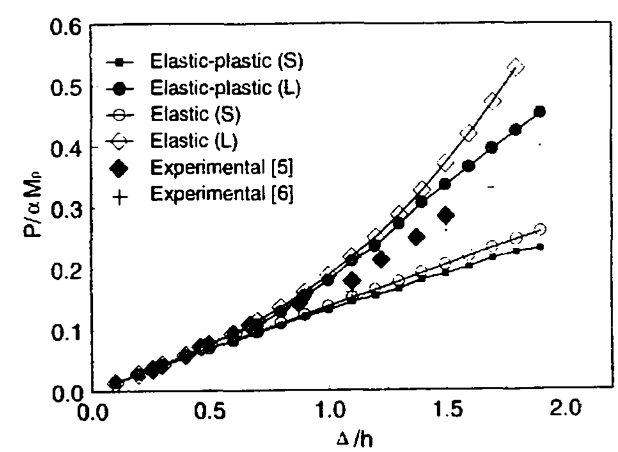

Fig. 8. Comparison between different load - punch displacement curves.

2. In stamping a circular plate the distribution of the contact stress between the plate and punch varies with the punch displacement. The maximum contact stress occurs at the plate centre initially and moves outwards when the plate is deformed further. A central gap between the punch and the plate will appear and will not disappear before coining.

3. The applicability of the small deflection theory of bending to plate stamping is more limited than is usually thought when an adequate prediction of the contact stress is required.

Appendix A. Nomenclature

C_{ep}	elastic-plastic stress-strain matrix
d_c	outer diameter of the contact zone
d_i	distance between the centre of the punch and the i-th node on the plate
e_k, e_R	the convergence indices for kinetic energy and residual force of the dynamic system
E	Young's modulus
g	gap between the plate and punch
h	thickness of the plate
M	bending moment
$\mathbf{M}$	diagonal mass matrix of the discrete system ($[m_{ii}^L]$)
M_p	fully plastic bending moment, $Yh^2/4$
N	membrane force
N_{max}	maximum iteration number with respect to fictitious time
N_{total}	total node number of the discrete system
n	number of iteration
P	total external load
q	normal contact pressure
R	radius of the circular plate
$\boldsymbol{R}$	vector of residual forces of the discrete system
R_p	radius of the hemispherical punch
r	radial coordinate
u, v, w	displacement components in x, y and z directions, respectively
$\boldsymbol{X}$	vector of solution of the discrete system
$\tilde{\boldsymbol{X}}^0$	initial vector for iteration
$\dot{\boldsymbol{X}}$	vector of fictitious velocity of the discrete system
Y	yield stress
z	direction normal to the mid-plane of the plate
α	non-dimensional parameter, $R^2/R_p h$
Δ	displacement of the punch
$\delta(...)$	a small increment of quantity (...)
ε	normal strain
ξ	critical node damping factor
η	proportional factor
ϕ	semi-angle of the conical die
μ	friction coefficient between the workpiece and the conical die
ν	Poisson's ratio
σ	normal stress
$\bar{\sigma}$	effective stress
Ψ	punch surface equation

Superscripts and subscripts

i	node i
J	the number of displacement step
L	indication of three perpendicular directions coincident with displacement u, v, and w, respectively
n	n-th iteration step
r, θ	r and θ directions

References

[1] W. Johnson and A.N. Singh, Springback in circular blanks, *Metallurgia*, *47* (1980) 275-280.

[2] T.X. Yu and W. Johnson, The press-brake bending of rigid/linear work-hardening plates, *Int. J. Mech. Sci.*, *23* (1981) 307-318.

[3] T.X. Yu, W. Johnson and W.J. Stronge, Stamping and springback of circular plates deformed in hemispherical dies, *Int. J. Mech. Sci.*, *26* (1984) 131-148.

[4] W.J. Stronge, M.P.F. Sutcliffe and T.X. Yu, Wrinkling of elastoplastic circular plates during stamping, *Exp. Mech.*, *26* (1986) 345-353.

[5] L.C. Zhang, T.X. Yu and R. Wang, Investigation of sheet metal forming by bending—part IV: bending and wrinkling of circular sheets pressed by a hemispherical punch, *Int. J. Mech. Sci.*, *31* (1989) 335-348.

[6] G. Lu and L.S. Ong, Study on the stamping of elastic plastic plates, *J. Mater. Process. Manufact. Sci.*, *2* (1994) 305-314.

[7] K. Kormi, D.C. Webb and R.A. Etheridge, FEM simulation of the pressing of a strip into a cylindrical die and of a circular plate into a hemispherical one and their comparison with experiment, *J. Mater. Process. Technol.*, *42* (1994) 463-473.

[8] M. Kadkhodayan and L.C. Zhang, A consistent DXDR method for elastic-plastic problems, *Int. J. Numer. Meth. Eng.*, *38* (1995) 2413-2431.